CrossMark click for updates

Mobile hydrogen carbonate acts as proton acceptor in photosynthetic water oxidation

Sergey Koroidov[a], Dmitriy Shevela[a,1], Tatiana Shutova[b], Göran Samuelsson[b], and Johannes Messinger[a,1]

[a]Department of Chemistry, Chemical Biological Centre and [b]Department of Plant Physiology, Umeå Plant Science Centre, Umeå University, S-90187 Umeå, Sweden

Edited by Pierre A. Joliot, Institut de Biologie Physico-Chimique, Paris, France, and approved March 4, 2014 (received for review December 13, 2013)

Cyanobacteria, algae, and plants oxidize water to the O_2 we breathe, and consume CO_2 during the synthesis of biomass. Although these vital processes are functionally and structurally well separated in photosynthetic organisms, there is a long-debated role for CO_2/HCO_3^- in water oxidation. Using membrane-inlet mass spectrometry we demonstrate that HCO_3^- acts as a mobile proton acceptor that helps to transport the protons produced inside of photosystem II by water oxidation out into the chloroplast's lumen, resulting in a light-driven production of O_2 and CO_2. Depletion of HCO_3^- from the media leads, in the absence of added buffers, to a reversible down-regulation of O_2 production by about 20%. These findings add a previously unidentified component to the regulatory network of oxygenic photosynthesis and conclude the more than 50-y-long quest for the function of CO_2/HCO_3^- in photosynthetic water oxidation.

carbon dioxide | bicarbonate | proton release | oxygen evolution | water splitting

Oxygenic photosynthesis in cyanobacteria, algae, and higher plants leads to the reduction of atmospheric CO_2 to energy-rich carbohydrates. The electrons needed for this process are extracted in a cyclic, light-driven process from water that is split into dioxygen (O_2) and protons. This reaction is catalyzed by a penta-μ-oxo bridged tetra-manganese calcium cluster (Mn_4CaO_5) within the oxygen-evolving complex (OEC) of photosystem II (PSII) (1–4). The possible roles of inorganic carbon, C_i ($C_i = CO_2, H_2CO_3, HCO_3^-, CO_3^{2-}$), in this process have been a controversial issue ever since Otto Warburg and Günter Krippahl (5) reported in 1958 that oxygen evolution by PSII strictly depends on CO_2 and therefore has to be based on the photolysis of H_2CO_3 ("*Kohlensäure*") and not of water. These first experiments were indirect and, as became apparent later, were wrongly interpreted (6–8). Several research groups followed up on these initial results and identified two possible sites of C_i interaction within PSII (reviewed in refs. 9–12). Functional and spectroscopic studies showed that HCO_3^- facilitates the reduction of the secondary plastoquinone electron acceptor (Q_B) of PSII by participating in the protonation of Q_B^{2-}. Binding of HCO_3^- (or CO_3^{2-}) to the nonheme Fe between the quinones Q_A and Q_B was recently confirmed by X-ray crystallography (3, 13, 14). Despite this functional role at the acceptor side, the very tight binding of HCO_3^- to this site makes it impossible for the activity of PSII to be affected by changing the C_i level of the medium; instead inhibitors such as formate need to be added to induce the acceptor-side effect (15). Consequently, the water-splitting electron-donor side of PSII has also been studied intensively (for recent reviews, see refs. 11 and 12). Although a tight binding of C_i near the Mn_4CaO_5 cluster is excluded on the basis of X-ray crystallography (3, 14), FTIR spectroscopy (16), and mass spectrometry (17, 18), the possibility that a weakly bound HCO_3^- affects the activity of PSII at the donor side remains a viable option (reviewed in refs. 10 and 19).

In the present study using higher plant PSII membranes, we specifically evaluate a recently suggested role of weakly bound HCO_3^-, namely, that it acts as an acceptor for, and transporter of, protons produced by water splitting in the OEC (20–22).

Results

Time-resolved isotope-ratio membrane-inlet mass spectrometry (TR-MIMS) allows simultaneous on-line detection of various dissolved gas molecules with high sensitivity. This method, in which the gas molecules contained in the sample enter the vacuum of the mass spectrometer via pervaporation through a gas-permeable membrane, is therefore ideally suited to test the effect and mechanism of HCO_3^- interaction with PSII (23, 24). The TR-MIMS experiments presented below were performed either in on-line or off-line mode. The commonly used on-line approach leads to a strong HCO_3^- depletion of the samples owing to the consumption of CO_2 by the mass spectrometer and the interconversion of all C_i species. In contrast, the off-line approach allows the experiments to be performed at well-defined HCO_3^- levels (ambient or depleted). The two techniques are illustrated schematically in Fig. 1.

Effects of Mild HCO_3^- Depletion on PSII Activity. To confirm that HCO_3^- is of functional relevance for photosynthetic water splitting under our mild HCO_3^--depletion conditions we monitored O_2 evolution of PSII by off-line TR-MIMS at ambient (C_i^+) and C_i-depleted conditions (C_i^-). In these experiments an approximately 20-fold reduction in C_i levels was achieved by bubbling sample solutions, electron acceptors, and $H_2^{18}O$ (97.6%) with CO_2-depleted air inside a sealed septum vial (25). The sample suspensions were then transferred into gas-tight syringes

Significance

Photosynthesis by cyanobacteria, algae, and plants sustains life on Earth by oxidizing water to the O_2 we breathe and by converting CO_2 into biomass we eat, burn, or use otherwise. Although O_2 production and CO_2 reduction are functionally and structurally well separated in photosynthetic organisms, there is a long debated role of CO_2/HCO_3^- in water oxidation. Here we demonstrate that HCO_3^- acts as mobile acceptor and transporter of protons produced by photosystem II, and that depletion of HCO_3^- leads to a reversible down-regulation of O_2 production. These findings add a previously unidentified component to the regulatory networks in higher plants, algae, and cyanobacteria and conclude the long quest for the function of CO_2/HCO_3^- in photosynthetic water oxidation.

Author contributions: S.K., D.S., T.S., G.S., and J.M. designed research; S.K. and D.S. performed research; J.M. conceived experiments; S.K., D.S., G.S., and J.M. analyzed data; and S.K., D.S., and J.M. wrote the paper.

The authors declare no conflict of interest.

This article is a PNAS Direct Submission.

Freely available online through the PNAS open access option.

[1]To whom correspondence may be addressed. E-mail: dmitriy.shevela@chem.umu.se or Johannes.Messinger@chem.umu.se.

This article contains supporting information online at www.pnas.org/lookup/suppl/doi:10.1073/pnas.1323277111/-/DCSupplemental.

Fig. 1. Schematic view of the on-line and off-line TR-MIMS setup. For on-line experiments PSII membranes were loaded into the home-built MIMS cell and degassed for 20–40 min until stable baselines for all detected gases were reached (*Lower Right*). This leads to a nearly complete depletion of the samples of C_i. The sample was then illuminated with xenon flashes or by continuous white light from a slide projector. In off-line measurements the PSII membranes were illuminated inside of gas-tight syringes, that is, at well-defined C_i levels (ambient or depleted), and then injected into buffer of identical composition and pH that was thoroughly degassed in the MIMS cell.

and illuminated with white light for 10 s to induce O_2 formation by water splitting in PSII. The O_2 production was assayed by injecting the sample into the MIMS cell that contained a buffer of the same composition and pH, but extremely low dissolved gas concentration owing to the constant removal of gas by the mass spectrometer via the membrane inlet. Comparison of the C_i^+ and C_i^- traces in Fig. 2 shows that the O_2 yield of the C_i^- sample is 20% lower than that of the C_i^+ sample. Reversibility of the effect was established by exposing C_i^- samples for 20 min to air before illumination in the syringe (C_i^{-+} samples). A similar inhibition was achieved if the C_i depletion was performed by bubbling with N_2, and a rapid (≤2 min) recovery was seen after C_i was added in absence of O_2 in form of $NaHCO_3$ powder (Fig. S1). These experiments confirm that HCO_3^- enhances the activity of PSII.

HCO_3^- Acts as Proton Acceptor. According to a recent proposal, the activating role of HCO_3^- on PSII demonstrated above may be caused by the ability of HCO_3^- to act as a base for protons produced by photosynthetic water oxidation (20–22). If this proposal is correct, then the transiently formed H_2CO_3 should decay according to Reaction **1** into water and CO_2:

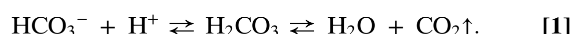

$$HCO_3^- + H^+ \rightleftarrows H_2CO_3 \rightleftarrows H_2O + CO_2\uparrow. \quad [1]$$

The CO_2 should then be released from PSII simultaneously with O_2 and must be detectable with TR-MIMS, because a maximum of four CO_2 per O_2 can be expected in the absence of any other proton acceptors. Fig. 3 displays the results obtained by using the conventional on-line approach, that is, by illuminating PSII suspensions inside the MIMS cell by a series of 50 saturating xenon flashes fired at 2 Hz. Because all mass peaks give the same results, Fig. 3 displays for clarity only the traces at mass-to-charge ratios of *m/z* 36 ($^{18}O_2$) and *m/z* 48 ($^{12}C^{18}O_2$), which detect CO_2 and O_2 with about the same high sensitivity (see Fig. S2 for the other traces). Under these conditions only light-induced O_2 evolution, and no CO_2 formation, is seen (Fig. 3, experiment 1). However, a 200-fold amplification of the CO_2 trace reveals a very small light-induced rise in the *m/z* 48 trace (Fig. 3, *Upper Inset*). Although small, the effect was reproducible and a light-induced heating artifact could be excluded by the inhibition of PSII turnover with the herbicide 3-(3,4-dichlorophenyl)-1,1-dimethylurea (DCMU) (Fig. 3, experiment 2). The more than 200-times smaller amplitude of the light-induced CO_2 production vs. O_2 evolution by PSII explains in part why the CO_2 formation by PSII was not reported previously. However, this very small CO_2 production may also call into question its biological relevance.

During the above on-line TR-MIMS experiments the samples need to be degassed in the MIMS cell for 20–40 min to reach a stable baseline. This leads to an almost complete removal of dissolved CO_2 from the solution (see data in Fig. 1). Owing to the interconversion of all C_i species (Reaction **1**) this also results in very low concentrations of HCO_3^- in the sample suspension (17), which may significantly reduce light-induced CO_2

Fig. 2. Dependence of water splitting in PSII on the C_i concentration of the medium. PSII membranes were illuminated with continuous white light of a slide projector for 10 s inside of gas-tight syringes and then injected into the MIMS cell. The C_i^+ trace was obtained at ambient C_i-concentration, whereas the C_i^- trace was recorded at a 20-times-reduced C_i concentration that was reached by purging PSII sample with CO_2 absorber (PCDA220M; Puregas). The reversibility was demonstrated by exposing a C_i^- sample for 20 min to air (C_i^{-+} trace). The final chlorophyll concentration was 50 μg (Chl) ml^{-1}, the $H_2^{18}O$-enrichment was 10%, and the medium contained 1 mM MES (pH 6.3), 15 mM NaCl, and 2 mM $K_3[Fe(CN)_6]$ and 0.25 mM 2-phenyl-*p*-benzoquinone (dissolved in DMSO) as electron acceptors. The average of two to three repeats is presented.

formation by PSII compared with in vivo conditions. We therefore performed off-line TR-MIMS experiments in which the dark-adapted PSII membranes were illuminated at ambient levels of CO_2/HCO_3^- in gas-tight syringes with 100 xenon flashes (2 Hz). For the detection of the light-induced gas formation the samples were then injected rapidly (<3 s) after the illumination into the MIMS cell containing the same buffer (but degassed). Fig. 4 displays the light-minus-dark difference signals of the $^{18}O_2$ and $^{12}C^{18}O_2$ gases (see original traces in Fig. S3). Under these more natural conditions, the CO_2 evolution reaches up to 20% of the O_2 evolution and can be clearly seen at the same sensitivity scale as O_2.

To compare the CO_2/O_2 ratios at different HCO_3^- concentrations in the sample buffer, we performed these off-line TR-MIMS experiments at pH 6.3 (Fig. 4*A*) and at pH 5.5 (Fig. 4*B*), which approximately corresponds to the luminal pH in photosynthetic organisms under illumination (26, 27). At pH 6.3 the CO_2 and HCO_3^- concentrations are about equal. When changing the pH of the solution to pH 5.5 under conditions that allow equilibration with air (open system), the concentration of dissolved CO_2 in the medium remains unchanged compared with pH 6.3, but the HCO_3^- concentration is reduced about six times (28) (*SI Text* and Table S1). Comparison of Fig. 4 *A* and *B* shows that the CO_2/O_2 ratio is more than two times lower at pH 5.5 compared with pH 6.3. Although the relative CO_2 evolution by PSII is not directly proportional to the HCO_3^- concentration, these data follow the trend expected if CO_2 is produced according to Reaction **1**.

The idea that HCO_3^- acts as proton acceptor was probed in air-saturated media by comparing light-induced CO_2 evolution at 10-fold different MES buffer concentrations (1 mM and 10 mM; Fig. 4*C*). MES at 200 mM was previously used to detect the proton release pattern of PSII by isotope-editing FTIR spectroscopy (29) and is therefore known to be a good proton acceptor for PSII that can outcompete HCO_3^- in its suspected role. A strongly reduced CO_2 and the same O_2 production were observed at 10 mM MES compared with 1 mM MES (Fig. 4 *C* and *D*), confirming this proposal. We note that this result excludes Warburg-type mechanisms (30) in which HCO_3^- acts directly or indirectly as a substrate of PSII, because for such mechanisms a buffer capacity independent CO_2/O_2 ratio is expected.

The competition between buffer and HCO_3^- for protons is further illustrated by the dotted traces in Fig. 4 *A* and *B*. They show that at 1 mM MES the CO_2/O_2 ratios are significantly lower if the PSII suspension is not injected rapidly (1–3 s) after illumination into the MIMS cells, but after waiting for some time (~1 min). This phenomenon reflects the back-conversion (Reaction **1**) of CO_2 into HCO_3^- by equilibration with water and proton acceptors such as side chains of proteins and lipids head groups of the sample or with MES according to their respective pK_a values (6.15 for MES and 6.38 for HCO_3^- at 20 °C) and the respective free base concentrations (410 μM MES^- vs. 12.8 μM HCO_3^-). It is noted that the O_2 levels do not change during the 1-min waiting time (Fig. S4). The CO_2 signals in Fig. 4 are therefore lower estimates of the initial production. We further illustrate this point in Fig. S5, where by using an automated flash-injection system we were able to observed CO_2/O_2 ratios >0.5 at 1 ms between illumination and injection. Importantly, the time-dependent equilibration shows that

Fig. 3. Simultaneous on-line TR-MIMS measurements of O_2 and CO_2 production by PSII. O_2 (blue traces) and CO_2 (green traces) evolution of dark-adapted spinach PSII membranes [0.3 mg (Chl)·mL^{-1}] induced by 50 saturating flashes at 2 Hz (trace 1). The arrows indicate the start of illumination. The inset displays the CO_2 evolution with 200-fold amplification. Trace 2 shows the same measurements after inhibition of PSII with the herbicide DCMU (80 μM). The amplitudes of the traces for CO_2 and O_2 can be directly compared, because our set-up detects both gases with nearly equal sensitivity. The measurements were performed in a buffer containing 3 mM MES (pH 6.3) in the presence of 1 mM $K_3[Fe(CN)_6]$ as exogenous electron acceptor. Final $H_2^{18}O$ enrichment was 10%. One representative result out of two to three repeats is presented.

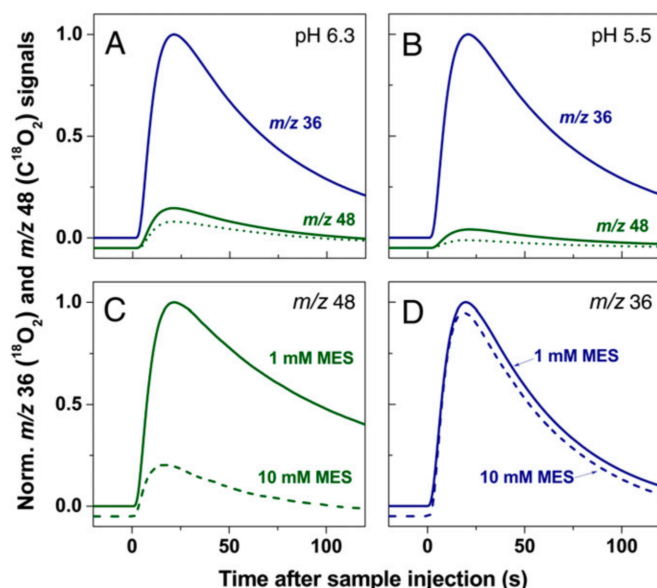

Fig. 4. Simultaneous off-line TR-MIMS measurements of O_2 and CO_2 production by PSII. Dark-adapted PSII membranes (1 mg Chl/mL) were illuminated inside of a gas tide syringe with 100 xenon flashes and then injected into the MIMS cell either as fast as possible with our current set up (<3 s, solid lines) or after 1 min (dotted line). Displayed are the light-minus-dark difference signals of O_2 (blue traces) and CO_2 (green traces), normalized to the amplitude of O_2 release (for original traces see Fig. S3). The amplitudes of the traces for CO_2 and O_2 can be directly compared, because our set-up detects both gases with nearly equal sensitivity. Conditions: (*A*) 1 mM MES, pH 6.3; (*B*) 1 mM MES, pH 5.5; (*C* and *D*) 1 mM MES (solid lines) or 10 mM MES (dashed lines), pH 6.3. In addition to MES, the medium contained 15 mM NaCl, 15% $H_2^{18}O$, and 2 mM $K_3[Fe(CN)_6]$ as electron acceptor. Zero levels are off set for clarity of presentation. In all panels the average of two to three repeats is presented.

HCO_3^- accepts protons produced by water splitting at sites within PSII that are not equally well accessible for the larger MES buffer molecules (i.e., that the CO_2 production is primarily a PSII-specific effect, rather than caused by a simple pH change of the medium).

Discussion

HCO_3^- Interaction with PSII in Vitro. The data in this study were obtained with isolated PSII membranes from spinach. This made it possible to study the effects of HCO_3^- on PSII activity without the need to consider indirect effects from related processes such as the carbon sequestration mechanisms (CCMs) operational in many algae and cyanobacteria (31). Our results clearly demonstrate that illumination of higher-plant PSII membranes with visible light induces both O_2 and CO_2 evolution, and that the yield of CO_2 depends both on the concentrations of HCO_3^- and MES in the sample suspension. Quantitation of the signals in Fig. 4*A* reveals the production of about four CO_2 molecules per PSII (*Methods*). Therefore, we can exclude the possibility that the light-induced CO_2 production is due to the release of HCO_3^- from its binding site at the nonheme iron. Collectively our data demonstrate conclusively that exchangeable HCO_3^- acts as a base for protons produced by PSII during water splitting.

Special pathways or channels have been discussed for guiding protons away from the water-splitting Mn_4CaO_5 cluster (32, 33). We show that HCO_3^- can compete for protons from water splitting with up to 300 times higher MES^- concentration (at 10 mM MES) and that the CO_2 yield observed is time-dependent (Fig. 4 and Fig. S5). We therefore propose that HCO_3^- is able to penetrate more deeply into PSII to accept protons than MES molecules, which are not present in vivo. Inspection of the 1.9-Å PSII crystal structure (3ARC code) reveals that HCO_3^- should indeed be able to penetrate easily into the entrance regions of all postulated channels; some channels are even wide and flexible enough to allow glycerol molecules to penetrate far inside (32, 33). In contrast, access to these channels for the even larger MES molecules would be more restricted. Once HCO_3^- accepts a proton it decomposes according to Reaction **1**, and the CO_2 is released from the channel and is either detected by MIMS or converted back to HCO_3^- by equilibration with water and buffer groups in the lumen, or with the artificially added MES buffer. This is illustrated schematically in Fig. 5. These equilibration processes likely lead to the delayed detection of CO_2 compared with O_2 that is visible in the on-line experiment displayed in Fig. 3.

We suggest that owing to the comparatively weak binding in the channels, which is required for the proposed function as mobile proton acceptor and carrier, HCO_3^- does not have a high enough occupancy at any particular site to be observable in the crystal structures. It is noted that in vivo the buffer capacity of the lumen of chloroplasts was estimated to be 0.8–1.0 mM (pH 6.4–8.1) and suggested to be due mostly to stationary groups such as proteins and lipid head groups (34), and not to mobile buffers such as MES added here at low concentrations to minimize the bulk pH changes. In vivo the role of HCO_3^- for the activity of PSII may therefore be even more pronounced than observed during the experiments shown in Fig. 2.

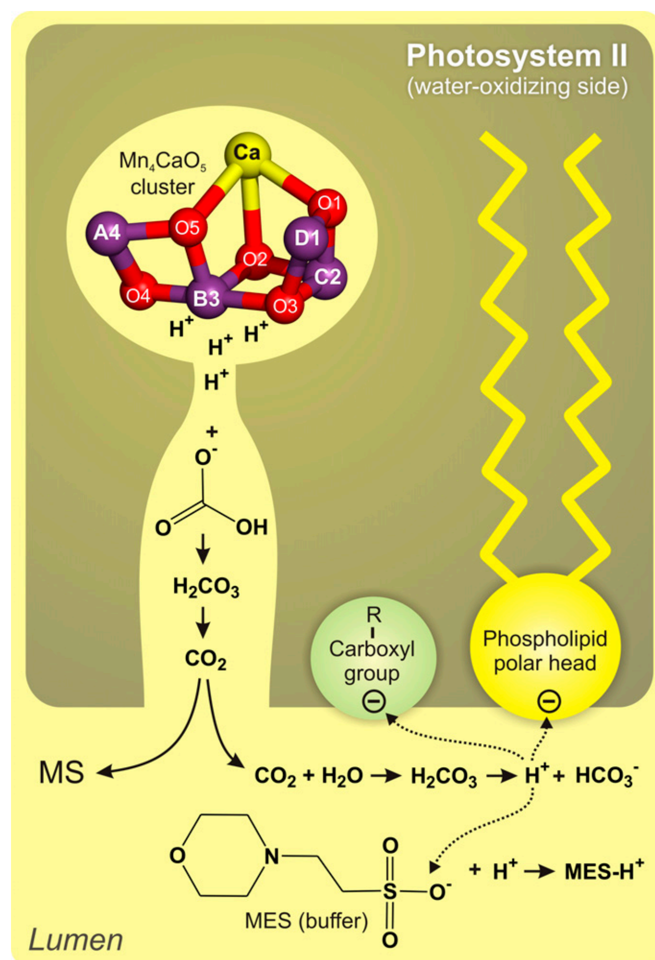

Fig. 5. Schematic representation of the function of HCO_3^- in PSII.

Biological Relevance. Higher plants take up CO_2 for carbon fixation by Rubisco via opening their stomata. Therefore, they do not possess special CCMs. In contrast, algae and cyanobacteria acquire CO_2 in the form of HCO_3^- from water, where its concentration is often very low. This requires CCMs that consist of several transporters to channel HCO_3^- through the various membranes, and of carbonic anhydrases that allow for efficient HCO_3^-/CO_2 interconversion (31, 35). The discovery of the PSII-bound Cah3 carbonic anhydrase (*cia3* gene product) in *Chlamydomonas reinhartii* (22, 36, 37) raised the question of whether this carbonic anhydrase together with HCO_3^- are required for PSII function, or whether they are part of the CCM mechanism that provides the nearby Rubisco with CO_2. Despite numerous experiments this point remained unresolved (21, 22, 35, 38). Although PSII membranes isolated from spinach also possess some carbonic anhydrase activity (6, 8), there is presently no evidence for a carbonic anhydrase directly connected to higher-plant PSII, and there is also no need for a CCM function (discussed above). Our finding that under continuous illumination the activity of PSII is nevertheless dependent on the HCO_3^- concentration of the buffer therefore demonstrates that HCO_3^- directly affects the activity of PSII. It is noted that the ability of HCO_3^- to capture protons will affect the H^+/e^- ratio owing to the loss of some CO_2 into the stroma, unless this is prevented by subsequent reformation of HCO_3^- via equilibration with stationary buffers in the lumen, which is strongly accelerated by carbonic anhydrases.

Although HCO_3^- cannot be viewed as a cofactor of water oxidation in PSII, our experiments do clearly demonstrate that it affects its activity. As such, a feedback loop can be envisioned between CO_2 fixation in the stroma and water oxidation at the luminal side of PSII: At high CO_2 levels in leaves the gas will be taken up into the alkaline stroma of the chloroplasts and trapped by conversion into HCO_3^-. Stromal carbonic anhydrases convert it back into CO_2 when the residual CO_2 is consumed by Rubisco for carbon fixation, or when it gets lost by diffusion into the lumen, where it will be also partially trapped as HCO_3^-. This leaching of CO_2 through the thylakoid membrane into the lumen allows PSII to "sense" the C_i level in the stroma. At high C_i levels in the chloroplasts many electrons can be used for CO_2 fixation, and HCO_3^- in the lumen activates PSII so that it produces electrons at maximum efficiency. In contrast, at low CO_2/HCO_3^- levels fewer electrons are needed, and the down-regulation of PSII by 20% (or more) helps to mitigate an overreduction of the plastoquinone pool, which reduces the risk of producing reactive oxygen species that are known to be damaging to enzymes involved in photosynthesis (39–41). Future studies will be needed to elucidate whether such a feedback loop is indeed operational.

Summary

The light-induced CO_2 formation by PSII and the dependence of CO_2 evolution on the concentrations of C_i and added buffer in the medium demonstrate conclusively that HCO_3^- acts as mobile proton acceptor of PSII. The data in Fig. 2 show that the lack of this component leads under "stress" (continuous strong light) to reduced oxygen evolution by PSII (21, 22). Because strictly alternating electron and proton removals from the OEC seem to be an inherent and crucial part of the mechanism of water oxidation in PSII (42, 43), it seems very likely that this function of HCO_3^- developed early during evolution and can be found in all O_2-evolving organisms (44). This dependence of PSII activity on HCO_3^- concentration may also allow for a feedback regulation with the Calvin–Benson–Bassham cycle, which uses the electrons and protons from water splitting for CO_2 reduction to biomass.

Methods

Sample Preparation. PSII membranes ("BBY" type) were prepared from fresh leaves of *Spinacia* (*S.*) *oleracea* following protocols described earlier (45, 46). Typical rates of O_2 evolution for spinach PSII membranes were 400–500 μmol $(O_2)\cdot mg\ (Chl)^{-1}\cdot h^{-1}$. After isolation, the PSII membranes were frozen by dropping small aliquots into liquid nitrogen. The samples were then stored at −80 °C until used. Before the measurements, the samples were thawed in the dark on ice and diluted to the desired concentrations with MES medium containing 200–400 mM sucrose, 35 mM NaCl, and 1–10 mM MES/NaOH at pH 6.3 (or 5.5).

TR-MIMS Measurements. TR-MIMS measurements were performed with an isotope ratio mass spectrometer (Finnigan^Plus XP; Thermo) that was connected via a dry ice/C_2H_5OH cooling trap to a home-built membrane-inlet cell of 150- or 175-μL volume (depending on stir bar used) (47). The sample in the cell was separated from the vacuum (3×10^{-8} bar) of the mass spectrometer via a 1-cm-diameter inlet that was covered by a 25-μm-thick silicon membrane (MEM-213; Mempro) resting on a porous Teflon support (Ø 10 mm). In the mass spectrometer the gases were ionized by electron impact and separated by a magnetic sector field into a seven-cup Faraday detector array for simultaneous detection of $^{16}O_2$ (*m/z* 32), $^{16}O^{18}O$ (*m/z* 34), $^{18}O_2$ and ^{36}Ar (*m/z* 36), ^{40}Ar (*m/z* 40), $^{12}C^{16}O_2$ (*m/z* 44), $^{12}C^{16}O^{18}O$ (*m/z* 46), and $^{12}C^{18}O_2$ (*m/z* 48). The simultaneous recording of argon (*m/z* 40) served as a control. The MIMS cell was thermostated to 20 °C. During the measurements the sample suspensions were stirred constantly at high speed with a magnetic stir bar. Before the assays the sample suspensions (or buffers) were degassed for 20–40 min until an only slightly sloping baseline was reached. On-line monitoring of light-induced O_2 and CO_2 evolutions (Fig. 3) was done by illumination of the dark-adapted PSII membranes inside the MIMS cell with a train of 50 short saturating flashes (2 Hz) provided by xenon flash lamp (LS-1130–4, ∼5-μs half-width; Perkin–Elmer). Off-line measurements of light-induced O_2 and CO_2 evolutions were performed by excitation of the dark-adapted PSII membranes inside a gas-tight 250-μL Hamilton syringe and subsequent injection of the illuminated sample into the cell filled with the thoroughly degassed buffer solution of the same composition and pH. For the experiments displayed in Fig. 4 50-μL PSII sample suspensions [1 mg $(Chl)\cdot mL^{-1}$] were illuminated with 100 xenon flashes (PS 302, 2 Hz, light pack FY-604 ∼15-μs half-width; EG&G). For controls, 50-μL aliquots of dark-adapted PSII sample suspensions were injected into the MIMS cell (Fig. S3). The light-induced O_2 and CO_2 signals were calibrated by the injection of defined volumes of air-equilibrated buffer (284 μM O_2 and 15.4 μM CO_2 at 20 °C, pH 5.0) into the same medium (www.engineeringtoolbox.com/oxygen-solubility-water-d_841.html and http://co2now.org/current-co2/co2-now/). The CO_2/PSII ratio was determined by dividing the calibrated CO_2 concentration by the PSII reaction center (RC) concentration, assuming 250 Chl/RC. The analysis of the MIMS spectra was performed by using Origin software.

CO_2/HCO_3^--Depletion Procedure and Monitoring of C_i Levels. C_i was removed from the PSII sample suspension containing $H_2^{18}O$ and electron acceptors by means of 30-min flushing with CO_2-free air that was generated by a Puregas PCDA220M instrument, in which compressed air is directed through a desiccant chamber containing an adsorbent material for CO_2. This C_i-depletion procedure led to a ∼20-fold decrease of the CO_2 level (∼0.8 μM) without decreasing the oxygen level compared with samples containing ambient CO_2 and O_2 levels owing to exposure to air (C_i^+ media; ∼15.4 μM). To avoid contamination of C_i-depleted (C_i^-) media with atmospheric CO_2, the depletion procedure and all following sample handling and incubation steps were performed inside sealed septum vials. This procedure resulted in our C_i^--depleted PSII membranes. For reversibility measurements the C_i^--depleted suspension of PSII membranes (∼80 μL) was incubated for 20 min in air. For a better equilibration with atmospheric CO_2, the sample suspensions were continuously stirred in a septum vial with an opened cap.

The CO_2 and O_2 concentrations in CO_2-depleted air were determined by monitoring the oxygen and carbon dioxide content of the C_i^+ and C_i^- sample solutions. For this, the 50-μL aliquots of the C_i^+ and C_i^- media were injected into degassed MES buffer (pH 6.3) in the MIMS cell.

ACKNOWLEDGMENTS. We thank Govindjee, A. Stemler, and V. V. Klimov for many stimulating discussions on bicarbonate effects over the years, G. Han for help with PSII sample preparation, U. Sauer and E. Sauer-Eriksson for discussions on the accessibility of PSII channels for HCO_3^-, W. Junge for valuable comments on the manuscript, and the Max Planck Institute for Chemical Energy Conversion for the loan of the isotope ratio mass spectrometer. Financial support was provided by Vetenskapsrådet (J.M. and G.S.), Energimyndigheten (J.M.), Kempe Stiftelse (J.M. and G.S.), the Strong Research Environment Solar Fuels (Umeå University), and the Artificial Leaf Project Umeå (Knut and Alice Wallenberg Foundation).

1. Lubitz W, Reijerse EJ, Messinger J (2008) Solar water-splitting into H_2 and O_2: Design principles of photosystem II and hydrogenases. *Energy Environ Sci* 1:15–31.
2. Yano J, et al. (2006) Where water is oxidized to dioxygen: Structure of the photosynthetic Mn_4Ca cluster. *Science* 314(5800):821–825.
3. Umena Y, Kawakami K, Shen J-R, Kamiya N (2011) Crystal structure of oxygen-evolving photosystem II at a resolution of 1.9 Å. *Nature* 473(7345):55–60.
4. Dau H, Zaharieva I (2009) Principles, efficiency, and blueprint character of solar-energy conversion in photosynthetic water oxidation. *Acc Chem Res* 42(12):1861–1870.
5. Warburg O, Krippahl G (1958) Hill-Reaktionen. *Z Naturforsch B* 13B(8):509–514.
6. Clausen J, Beckmann K, Junge W, Messinger J (2005) Evidence that bicarbonate is not the substrate in photosynthetic oxygen evolution. *Plant Physiol* 139(3):1444–1450.
7. Radmer R, Ollinger O (1980) Isotopic composition of photosynthetic O_2 flash yields in the presence of $H_2{}^{18}O$ and $HC^{18}O_3^-$. *FEBS Lett* 110(1):57–61.
8. Hillier W, et al. (2006) Quantitative assessment of intrinsic carbonic anhydrase activity and the capacity for bicarbonate oxidation in photosystem II. *Biochemistry* 45(7): 2094–2102.
9. Stemler AJ (2002) The bicarbonate effect, oxygen evolution, and the shadow of Otto Warburg. *Photosynth Res* 73(1-3):177–183.
10. Van Rensen JJS, Klimov VV (2005) Bicarbonate interactions. Photosystem II The Light-Driven Water: Plastoquinone Oxidoreductase, *Advances in Photosynthesis and Respiration*, eds Wydrzynski T, Satoh K (Springer, Dordrecht), Vol 22, pp 329–346.
11. Shevela D, Eaton-Rye JJ, Shen J-R, Govindjee (2012) Photosystem II and the unique role of bicarbonate: A historical perspective. *Biochim Biophys Acta* 1817(8):1134–1151.
12. McConnell IL, Eaton-Rye JJ, Van Rensen JJS (2012) Regulation of photosystem II electron transport by bicarbonate. *Photosynthesis: Plastid Biology, Energy Conversion and Carbon Assimilation*, eds Eaton-Rye JJ, Tripathy BC, Sharkey TD (Springer, Dordrecht), pp 475–500.
13. Cox N, et al. (2009) The semiquinone-iron complex of photosystem II: structural insights from ESR and theoretical simulation; evidence that the native ligand to the non-heme iron is carbonate. *Biophys J* 97(7):2024–2033.
14. Guskov A, et al. (2010) Recent progress in the crystallographic studies of photosystem II. *ChemPhysChem* 11(6):1160–1171.
15. Govindjee (1993) Bicarbonate-reversible inhibition of plastoquinone reductase in photosystem II. *Z Naturforsch* C 48(3-4):251–258.
16. Aoyama C, Suzuki H, Sugiura M, Noguchi T (2008) Flash-induced FTIR difference spectroscopy shows no evidence for the structural coupling of bicarbonate to the oxygen-evolving Mn cluster in photosystem II. *Biochemistry* 47(9):2760–2765.
17. Shevela D, Su JH, Klimov V, Messinger J (2008) Hydrogencarbonate is not a tightly bound constituent of the water-oxidizing complex in photosystem II. *Biochim Biophys Acta* 1777(6):532–539.
18. Ulas G, Olack G, Brudvig GW (2008) Evidence against bicarbonate bound in the O_2-evolving complex of photosystem II. *Biochemistry* 47(10):3073–3075.
19. Dasgupta J, Ananyev GM, Dismukes GC (2008) Photoassembly of the water-oxidizing complex in photosystem II. *Coord Chem Rev* 252(3-4):347–360.
20. Ananyev G, Nguyen T, Putnam-Evans C, Dismukes GC (2005) Mutagenesis of CP43-arginine-357 to serine reveals new evidence for (bi)carbonate functioning in the water oxidizing complex of Photosystem II. *Photochem Photobiol Sci* 4(12):991–998.
21. Shutova T, et al. (2008) The photosystem II-associated Cah3 in *Chlamydomonas* enhances the O_2 evolution rate by proton removal. *EMBO J* 27(5):782–791.
22. Villarejo A, et al. (2002) A photosystem II-associated carbonic anhydrase regulates the efficiency of photosynthetic oxygen evolution. *EMBO J* 21(8):1930–1938.
23. Beckmann K, Messinger J, Badger MR, Wydrzynski T, Hillier W (2009) On-line mass spectrometry: Membrane inlet sampling. *Photosynth Res* 102(2-3):511–522.
24. Shevela D, Messinger J (2013) Studying the oxidation of water to molecular oxygen in photosynthetic and artificial systems by time-resolved membrane-inlet mass spectrometry. *Front Plant Sci* 4:473.
25. Shevela D, et al. (2013) Efficiency of photosynthetic water oxidation at ambient and depleted levels of inorganic carbon. *Photosynth Res* 117(1-3):401–412.
26. Takizawa K, Cruz JA, Kanazawa A, Kramer DM (2007) The thylakoid proton motive force in vivo. Quantitative, non-invasive probes, energetics, and regulatory consequences of light-induced *pmf*. *Biochim Biophys Acta* 1767(10):1233–1244.
27. Tikhonov AN, et al. (2008) Spin-probes designed for measuring the intrathylakoid pH in chloroplasts. *Biochim Biophys Acta* 1777(3):285–294.
28. Stumm W, Morgan JJ (1995) *Aquatic Chemistry: Chemical Equilibria and Rates in Natural Waters* (Wiley, New York), 3rd Ed, p 1040.
29. Suzuki H, Sugiura M, Noguchi T (2009) Monitoring proton release during photosynthetic water oxidation in photosystem II by means of isotope-edited infrared spectroscopy. *J Am Chem Soc* 131(22):7849–7857.
30. Metzner H (1978) *Photosynthetic Oxygen Evolution* (Academic, London).
31. Badger MR, Price GD (2003) CO_2 concentrating mechanisms in cyanobacteria: Molecular components, their diversity and evolution. *J Exp Bot* 54(383):609–622.
32. Gabdulkhakov A, et al. (2009) Probing the accessibility of the $Mn_{(4)}Ca$ cluster in photosystem II: Channels calculation, noble gas derivatization, and cocrystallization with DMSO. *Structure* 17(9):1223–1234.
33. Ho FM (2008) Uncovering channels in photosystem II by computer modelling: Current progress, future prospects, and lessons from analogous systems. *Photosynth Res* 98(1-3):503–522.
34. Junge W, Ausländer W, McGeer AJ, Runge T (1979) The buffering capacity of the internal phase of thylakoids and the magnitude of the pH changes inside under flashing light. *Biochim Biophys Acta* 546(1):121–141.
35. Van Hunnik E, Sultemeyer D (2002) A possible role for carbonic anhydrase in the lumen of chloroplast thylakoids in green algae. *Funct Plant Biol* 29(2-3):243–249.
36. Karlsson J, et al. (1998) A novel alpha-type carbonic anhydrase associated with the thylakoid membrane in *Chlamydomonas reinhardtii* is required for growth at ambient CO_2. *EMBO J* 17(5):1208–1216.
37. van Hunnik E, et al. (2001) Identification and localization of a thylakoid-bound carbonic anhydrase from the green algae *Tetraedron minimum* (Chlorophyta) and *Chlamydomonas noctigama* (Chlorophyta). *Planta* 212(3):454–459.
38. Hanson DT, Franklin LA, Samuelsson G, Badger MR (2003) The *Chlamydomonas reinhardtii cia3* mutant lacking a thylakoid lumen-localized carbonic anhydrase is limited by CO_2 supply to rubisco and not photosystem II function in vivo. *Plant Physiol* 132(4):2267–2275.
39. Gill SS, Tuteja N (2010) Reactive oxygen species and antioxidant machinery in abiotic stress tolerance in crop plants. *Plant Physiol Biochem* 48(12):909–930.
40. Pospísil P (2009) Production of reactive oxygen species by photosystem II. *Biochim Biophys Acta* 1787(10):1151–1160.
41. Rutherford AW, Osyczka A, Rappaport F (2012) Back-reactions, short-circuits, leaks and other energy wasteful reactions in biological electron transfer: Redox tuning to survive life in $O_{(2)}$. *FEBS Lett* 586(5):603–616.
42. Siegbahn PEM (2009) Water oxidation in photosystem II: Oxygen release, proton release and the effect of chloride. *Dalton Trans* 45(45):10063–10068.
43. Klauss A, Haumann M, Dau H (2012) Alternating electron and proton transfer steps in photosynthetic water oxidation. *Proc Natl Acad Sci USA* 109(40):16035–16040.
44. Dismukes GC, et al. (2001) The origin of atmospheric oxygen on Earth: The innovation of oxygenic photosynthesis. *Proc Natl Acad Sci USA* 98(5):2170–2175.
45. Berthold DA, Babcock GT, Yocum CF (1981) A highly resolved, oxygen-evolving photosystem II preparation from spinach thylakoid membranes. *FEBS Lett* 134:231–234.
46. Ono T-A, Inoue Y (1983) Mn-preserving extraction of 33-, 24- and 16-kDa Proteins from O_2-evolving PS II particles by divalent salt-washing. *FEBS Lett* 164(2):255–260.
47. Messinger J, Badger MR, Wydrzynski T (1995) Detection of *one* slowly exchanging substrate water molecule in the S_3 state of photosystem II. *Proc Natl Acad Sci USA* 92(8):3209–3213.